

Investigation of Hole-Edge Cracking in TRIP 780 Using the Structural Component Bend Test

Hyunok Kim, Menachem Kimchi
Edison Welding Institute

Abstract

Local failure such as hole-edge cracking is often observed in forming advanced high-strength steels (AHSS). Numerical prediction of this local failure is challenging for simulation engineers to evaluate stamping and crash performances of materials. Finite element method (FEM) modelling requires additional input data, “failure criteria” to predict the local failures of material, in addition to the material flow stress data input for simulation. This paper presents the procedure to develop the hole-edge failure criteria using various formability tests and to design a component bend test structure to evaluate the hole-edge failures of AHSS structures. A local-strain-based failure criterion and a stress-triaxiality-based failure criterion were developed and implemented in a FEM simulation code to predict hole-edge failures in component bend tests. The holes were prepared using two different methods: mechanical punching and water-jet cutting. In the component bend tests, the water-jet trimmed hole showed delayed fracture at the hole-edges, while the mechanical punched hole showed early fracture as the bending angle increased. In comparing the simulation and test results, the load-displacement curve, the displacement at the onset of cracking, and the final crack shape/length were used. Both failure criteria showed good correlations with experimental observations, while the conventional tensile-test-based failure criterion resulted in over-prediction of the local formability of the hole-edge during bending and stretching. Both failure criteria also enable the numerical model to differentiate between the local formability limit of mechanical-punched and water-jet-trimmed holes. The stress triaxiality-based criterion also allowed the prediction of the failure in the bucking area where typical ductile failure is observed. The failure criteria and static bend test developed here are useful to evaluate the local failure at a structural component level for automotive crash tests.

Introduction

Hole-edge cracking is observed during plastic deformations in stamping of advanced high-strength steels (AHSS) and vehicle crash tests. Due to the complex nature of edge fracture behavior, finite-element (FE) modeling with conventional material model/data has had only limited success for predicting edge cracking. There are several important factors which influence on hole-edge cracking, including:

- Sheet material properties
- Edge quality of hole from punching
- Pre-strains on the edge caused by trimming or punching
- Burr formation (up or down with respect to a moving punch).

Background

Research in the area of hole-edge cracking prediction is actively ongoing. Two different approaches include more complicated modeling techniques by either correlation of FE simulation results of blanking/piercing with stamping [1], or conducting numerical modeling to explicitly consider the volume fraction of martensite and ferrite in the dual-phase microstructure [2, 3]. However, these approaches may be limited for the direct use in industry forming simulations, due to the higher computation cost and unknown parameters that the FE model cannot take into account, such as hole-edge imperfections (e.g., micro-cracks remained on hole-edge after punching) and microstructure characteristics (banding width and micro-void areas, etc.). The stress-triaxiality-based failure model to predict the failures in deep-drawing TRIP 700 material and bending the automotive structural component [4]. Compared to these complicated models, simpler prediction models were recently introduced [5, 6, 7]. A regression model was developed to handle all these unknown parameters in the hole-tensile test and hole-expansion test (HET) [5]. A simple ductile damage model was used to predict edge cracking in the bow-tie tensile test and HET [6]. A stress-strain based damage model was used to predict the local shear fracture during draw-bending of AHSS [7]. To account for macro-crack formation in FE simulations of HET, recently an inverse calibration method based on a damage model utilizing a triaxiality-dependent fracture criterion and hardening behavior was developed [8]. Therefore, for a given sheet material (including material properties and microstructure) and trimming process (punching, water-jet cutting, and laser cutting), a unique number or a small range of critical damage values that is the energy consumed to failure can be determined. With this background, it is desirable to develop a simple and practical failure model for industry applications for FE modeling of stamping and vehicle crash tests.

Objective

The primary objective of this study was to predict the hole-edge failures for AHSS structural components. The specific objectives are to:

- Develop a component bend test (i.e., the structure design and test conditions) to evaluate the hole-edge failures
- Predict hole-edge failure by using FE simulations with reliable failure criteria.

The Failure Criteria for Hole-Edge Cracking

The hole-edge failure criteria were determined by using different local formability testing (LFT) methods and FEM model. **Figure 1** illustrates the flow chart to determine the failure map and its application for component bend simulations. Four different LFT methods such as a tensile, hole-tensile and a plane-strain shear and the hole expansion tests were used to characterize the effects of material properties and trimming methods on the hole-edge failures. Experimental results were analyzed by using FEM simulations to calculate the local strain, damage value and stress-triaxiality (i.e., a ratio of equivalent stress and mean stress). From experimental and simulation models, two different failure criteria: a local-strain-based damage model and a stress-triaxiality-based failure model were determined. The failure models were used to design the component bend test and predict the hole-edge failures observed in the component bend test.

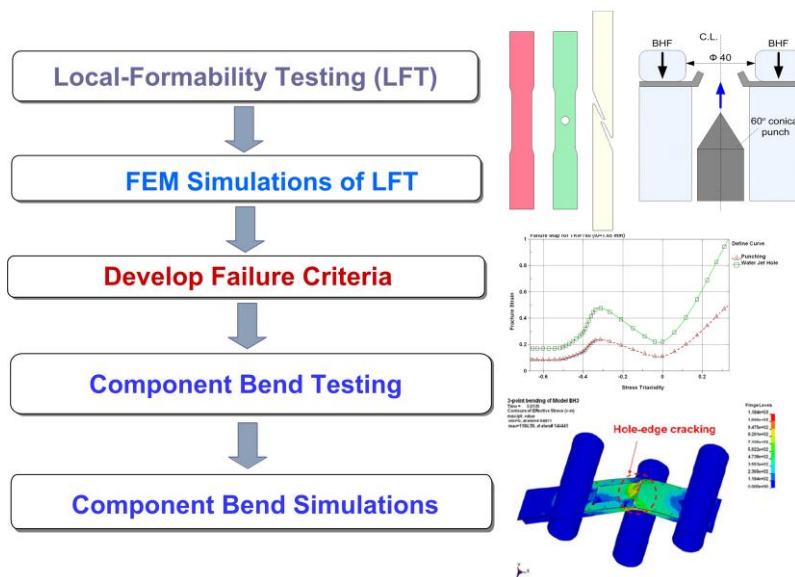


Figure 1: Flow chart to determine the failure map

The failure map was constructed with the local strains and different stress triaxiality calculated from FE simulations of various local-formability tests. The detailed procedure to construct the failure map is available in [4]. The CDV for TRIP 780 material was determined for different trimming conditions. Furthermore, two different failure maps were constructed for the punched-hole and water-jet-cut-hole cases. Both failure criteria were implemented for LS-DYNA simulations with MAT_224 as shown in **Figure 2**. In the stress-triaxiality based failure criteria, the failure strain varies with the stress triaxiality, while the local-strain based damage model has a constant failure strain as shown in **Figure 2**. When the strain of FE model reaches this failure strain, the element at failure strains starts eroding in LS-DYNA, which emulates the crack initiation and propagation in experiments.

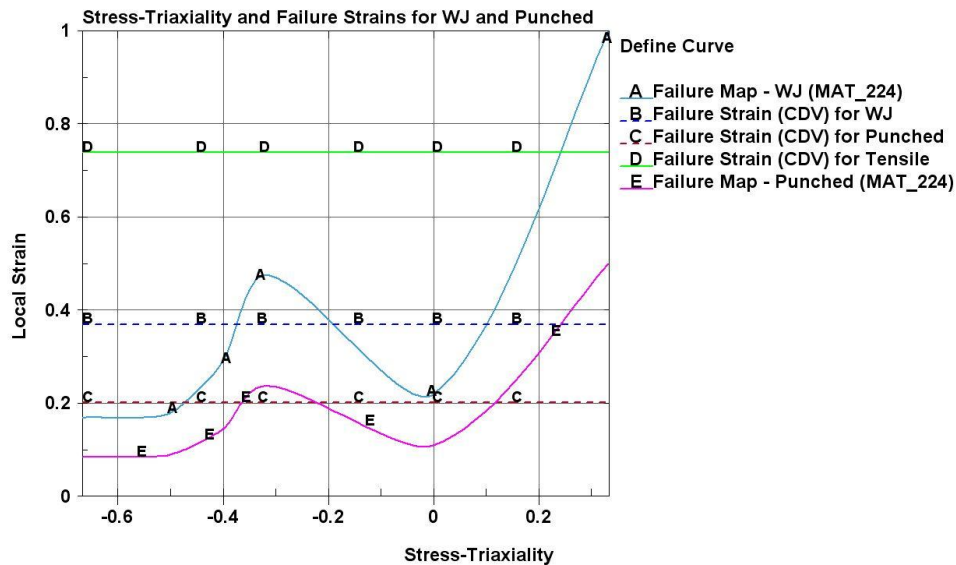


Figure 2: Failure map and criteria defined for FEM simulations for bending of the structural part

Design of the Component Bend Test

A component bend test was developed by conducting preliminary FE simulations of various hat-shaped structure designs by bench-marking other designs available in literature [9, 10]. Different locations and sizes of hole and spot welds were investigated to obtain reproducible hole-edge failures in the test.

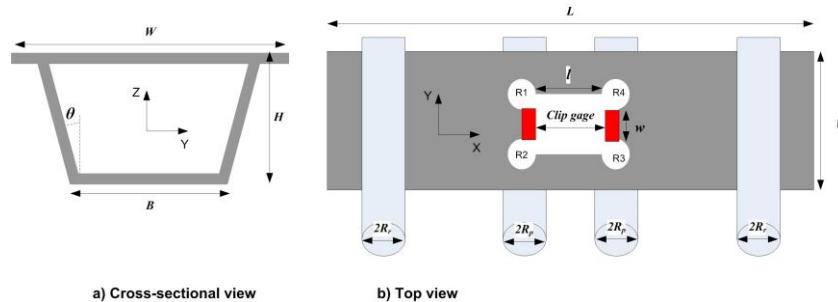


Figure 3: Schematic of the component structure and a bending configuration

Figure 4 illustrates the procedure to optimize key design parameters in the hat-structure geometry and bending configuration. A series of spot weld models were defined on the flange of a lower channel as shown in **Figure 5**. A weld-pitch of 25-mm was used and individual weld nugget model was defined to have 6-mm diagonal length and 1.65-mm thickness based on previous welding simulation experiences.

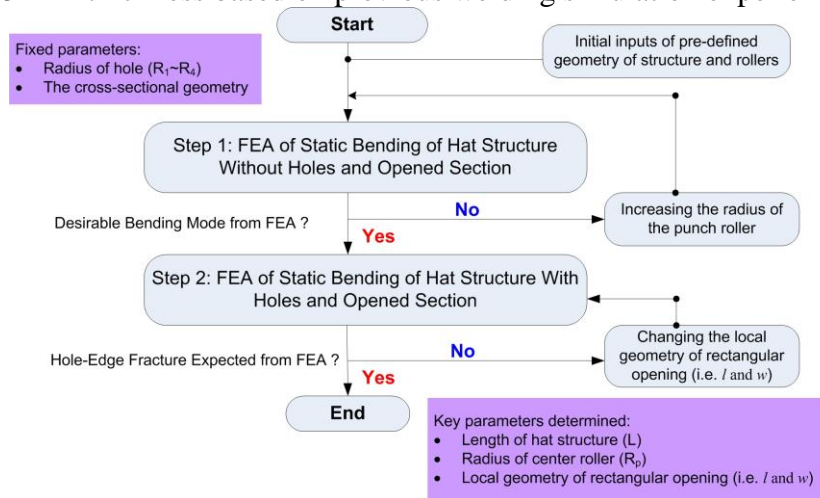


Figure 4: A flow chart of the component design using FEA

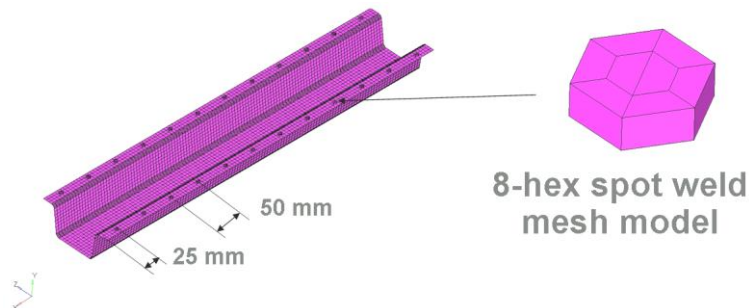


Figure 5: FE model of a lower channel part and a spot weld model

Experimental Results

Component bending tests were conducted at the MTS machine (300-kN capacity) and **Figure 6** shows the testing setup. During the test, the high-resolution camera recorded the hole-edge failure as the upper ram moved down and the structure is bent.

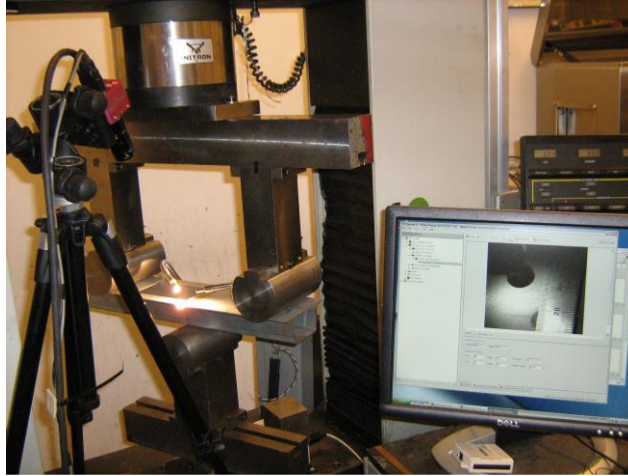


Figure 6: A 3-pt. bend test for AHSS structures

The component has a rectangular opening with four corner holes that were trimmed by punching or water-jet trimming. The lower hat-shaped channel was bent by using a press-brake machine. Finally, a top plate and a lower channel section were spot welded (e.g., 6-mm spot weld nugget diameter). The same TRIP 780 material was used for the entire component structure. During the test, the load-displacement curve was measured and synchronized with a high-resolution video camera monitoring the hole-edge region. Testing was conducted up to 120-mm stroke.

Test results were summarized in Table 1. The punched structure samples showed the edge cracking in a lower stroke (e.g. 30~40-mm) compared to the water-jet structure samples and this resulted that the punched samples gave 5-10 mm larger crack length compared to the water jet samples at the final stroke (i.e. 120-mm). **Figure 7** shows both punched and water jet samples tested. The overall bend angles were similar between the punched and the water-jet-trimmed structures. However, the punched case showed more severe cracks at two trimmed holes compared to the water-jet case.

Table 1: Summary of experimental results

Sample No.	Stroke at the start of cracking	Maximum Force
WJ-1	87 mm	19.41 kN
WJ-2	95 mm	19.27 kN
WJ-3	100 mm	19.35 kN
P-4	65 mm	19.31 kN
P-5	60 mm	19.33 kN
P-6	57 mm	19.23 kN

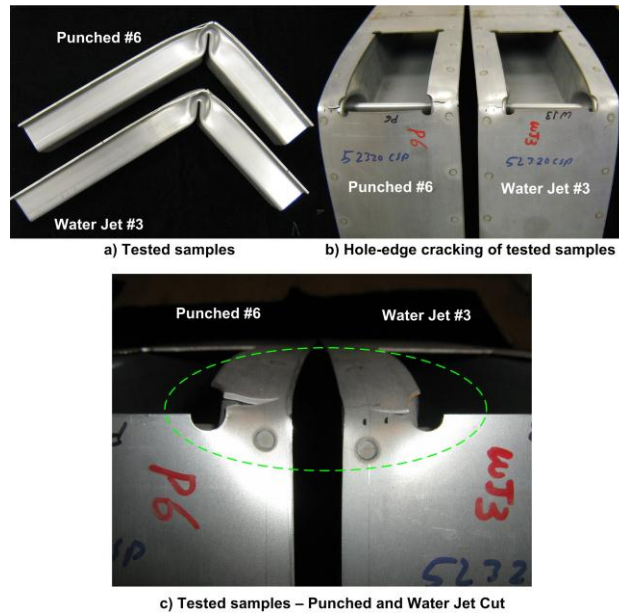


Figure 7: Tested component structures

FEM Results

Figure 8 shows the FE model for 3-point bend testing. A commercial FEM code, LS-DYNA was used for simulations. The fine mesh (2-mm) was used for the areas near the hole-edges and the remaining areas were meshed with 5-mm elements. The rollers were meshed with 4-mm elements uniformly. When the local strain reaches the limit strain, the element erosion is initiated as shown in **Figure 9**, and they are propagated to neighboring elements.

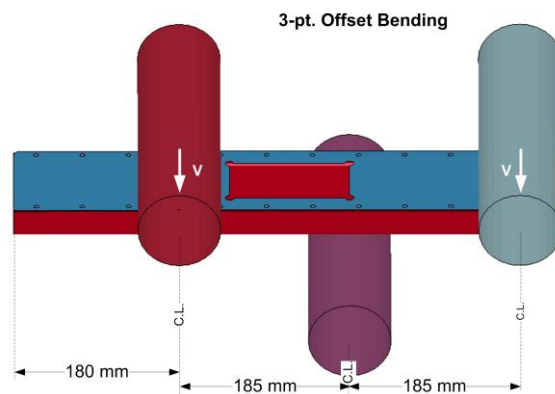


Figure 8: Testing configuration of a component bend test

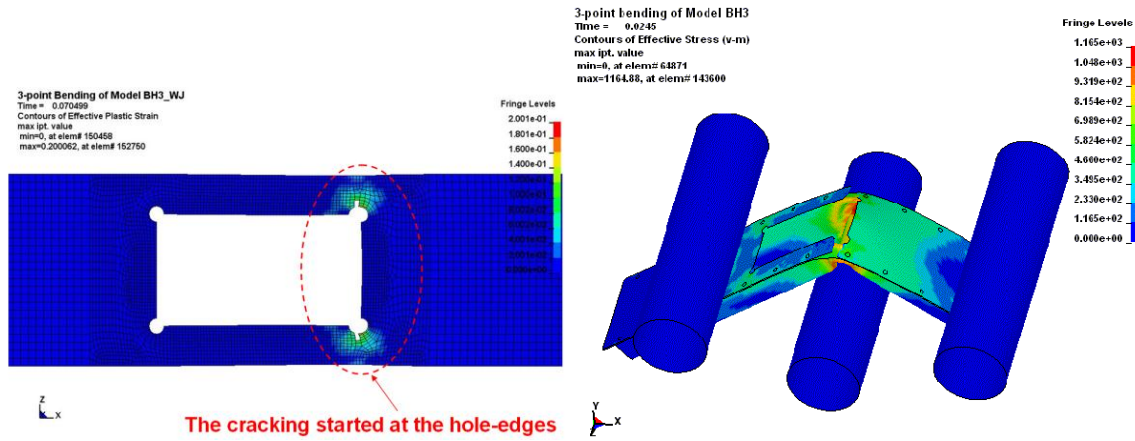


Figure 9: FEM predictions of the initiation of the hole-edge cracking (left) and the final fractured structure with the effective stress contour (right)

FEM simulations were conducted with the local strain-based damage model and the stress-triaxiality-based failure map (Figure 2). Compared to the test results of the punched case, the local-strain-based damage model gave better correlations than the stress triaxiality based failure map in terms of severity of cracking (Figure 10) as well as the critical stroke at the onset of hole-edge cracking as shown Figure 11.

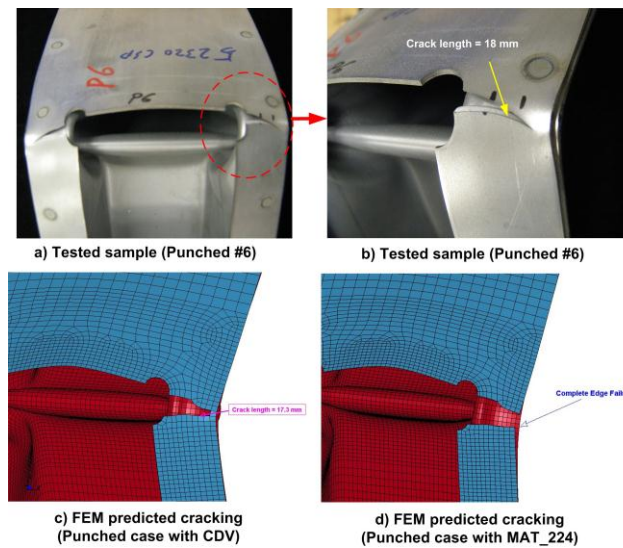


Figure 10: Comparison of edge-failure shapes between the experiment and FEM predictions with different failure criteria

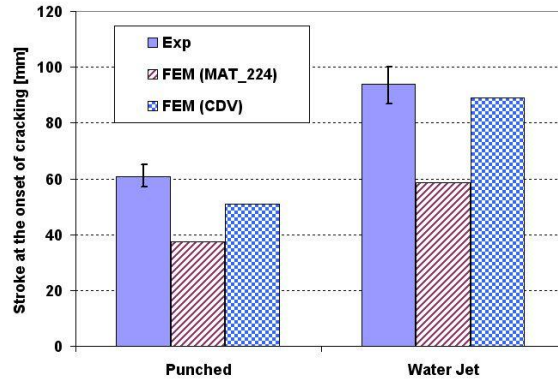


Figure 11: Comparison of the critical stroke at the onset of hole-edge cracking

The stress triaxiality and local strain were compared for two different failure criteria of punched and water-jet cases (**Figure 12**). The local strain value (0.74) from the ductile failure of a normal tensile test showed no edge failure and the local strain exceeded the boundary of failure strain limit that were determined by other failure criteria.

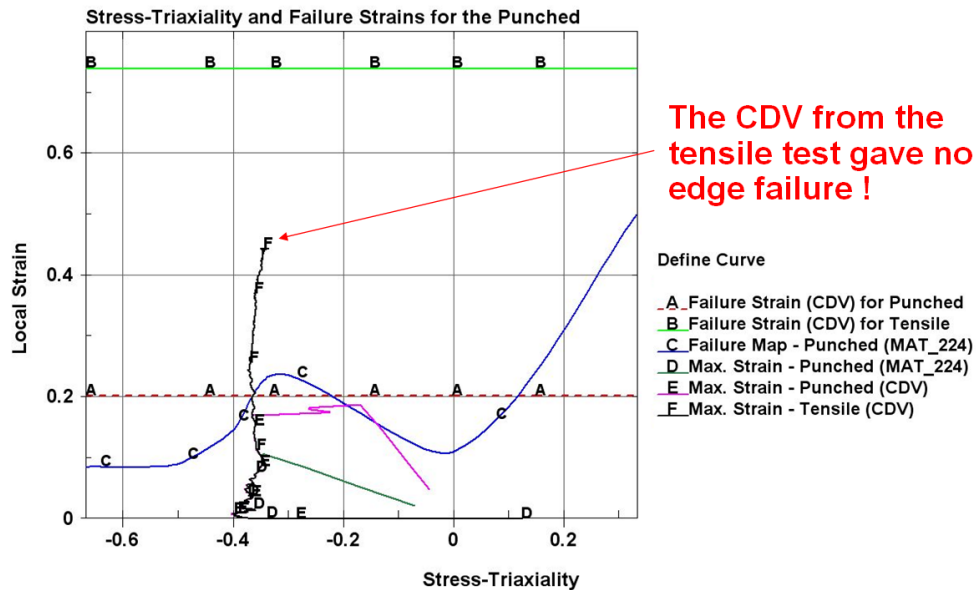


Figure 12: FEM predictions of the stress triaxiality and local strain with the different failure criteria for the punched case

Discussions

In this study, different trimming methods such as a mechanical punching and a water-jet cutting were used to make the hole of specimens remain different residual stresses and damages at the hole-edge and this difference can result in different behaviour of hole-edge failure in secondary forming and crash tests. A local-strain based failure model was determined by using the CDV for different trimmed edge quality. This model was evaluated for FE simulations of various tests and it showed the better predictions of hole-edge failures compared to the complex failure map that was established by considering the stress triaxiality. Therefore, to be able to reliably apply the complex stress triaxiality based model for the large scale crash model, a further study on stress triaxiality based failure model should be followed as a future work.

Conclusions

The following conclusions can be summarized from this study.

- A new methodology was able to evaluate the quality of hole edge with different trimming methods and also quantify the damage/local strain remained from those trimming processes.
- The punched hole showed the hole-edge failure at a lower strain compared to water-jet cutting.
- The local-strain based failure criterion gave better correlations with experiments than the stress-triaxiality based failure criterion. A failure map based on the stress-triaxiality and local strain is useful to predict the hole-edge failure.

References

1. R. Wiedenmann, P. Sartkulvanich, T. Altan, Finite element analysis on the effect of sheared edge quality in blanking upon hole expansion of advanced high strength steel, *International Deep Drawing Research Group (IDDRG) 2009 International Conference*, Golden, CO, United States.
2. X. Sun, K.S. Choi, Effects of AHSS Microstructure Inhomogeneity on Strain Localization, *Shear Fracture Technical Progress Review*, Auto/Steel Partnership, Sept., 10, 2008, Southfield, MI, United States.
3. X. Wu, C. Xie, H. Bahmanpour, Flange shear affected zone study, *Shear Fracture Technical Progress Review*, Auto/Steel Partnership, Sept, 10, 2008, Southfield, Michigan
4. D.Z. Sun, F. Andrieux, M. Feucht, Damage modeling of a TRIP steel for integrated simulation from deep drawing to crash, *7th European LS-DYNA Conference*, May 14-15, 2009, Salzburg, Austria.
5. K. Watanabe, M. Tachibana, K. Koyanagi, K. Motomura, Simple Prediction Method for the Edge Fracture of Steel Sheet during Vehicle Collision (1st report) – Evaluation of Fracture Limit from the Edge using Small-Sized Test Pieces, *LS-DYNA Conference*. 2006.
6. J.S. Lee, Y.K. Ko, H. Huh, H.K. Kim, S.H. Park, Evaluation of Hole Flangeability of Steel Sheet with Respect to the Hole Processing Condition, *Engineering Plasticity and its Applications* 340-341, 2007, pp. 665-670.
7. H. Kim, A.R. Bandar, Y. Yang, J.H. Sung, R.H. Wagoner, Failure Analysis of Advanced High Strength Steels (AHSS) During Draw Bending, International Deep Drawing Research Group, *IDDRG 2009 International Conference*, Golden, CO, United States.
8. K. Chung, N. Ma, T. Park, D. Kim, D. Yoo, C. Kim, A modified damage model for advanced high strength steel sheets, *International Journal of Plasticity*, Article In Press, 2011
9. N. Kojima, K. Fukui, N. Mizui, Improvement in Bending Crashworthiness of Hat-Shape Columns by using High Strength Steel Sheets, *40th Mechanical Working and Steel Processing Conference*, 1998, Pittsburgh, PA, United States.
10. K. Koyanagi, K. Motomura, Simple Prediction Method for the Edge Fracture of Steel Sheet during Vehicle Collision (2nd report), *LS-DYNA Conference 2006*, Anwenderforum, Ulm.